ELSEVIER

Nanomedicine: Nanotechnology, Biology, and Medicine
xx (xxxx) xxx

nanomedicine
Nanotechnology, Biology, and Medicine

nanomedjournal.com

Graphical Abstract

Nanomedicine: Nanotechnology, Biology, and Medicine xxx (2021) xxx–xxx

Tyrosine-modified linear PEIs for highly efficacious and biocompatible siRNA delivery *in vitro* and *in vivo*

Michael Karimov[a], Marion Schulz[a], Tim Kahl[a], Sandra Noske[a], Malgorzata Kubczak[b], Ines Gockel[c], René Thieme[c], Thomas Büch[a], Anja Reinert[d], Maksim Ionov[b], Maria Bryszewska[b], Heike Franke[e], Ute Krügel[e], Alexander Ewe[a], Achim Aigner[a,*]

[a]*Rudolf-Boehm-Institute for Pharmacology and Toxicology, Clinical Pharmacology, Leipzig University, Faculty of Medicine, Leipzig, Germany*
[b]*Department of General Biophysics, University of Łódź, Łódź, Poland*
[c]*Department of Visceral, Transplant, Thoracic and Vascular Surgery, University Hospital Leipzig, Leipzig, Germany*
[d]*Faculty of Veterinary Medicine, Institute of Anatomy, Histology and Embryology, Leipzig University, Leipzig, Germany*
[e]*Rudolf-Boehm-Institute for Pharmacology and Toxicology, Leipzig University, Faculty of Medicine, Leipzig, Germany*[f]

For therapeutic siRNA delivery, we generated and analyzed a set of small linear polyethylenimines bearing tyrosine modifications (LP*x*Y). Substantially enhanced siRNA delivery and knockdown efficacy, favorable physicochemical nanoparticle properties, very high biocompatibility and therapeutic efficacy were observed *in vitro* and in different tumor models *in vivo*.

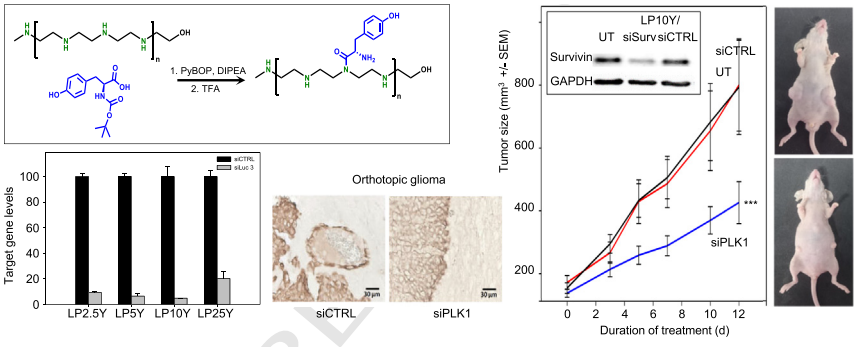

Please cite this article as: Karimov M., et al., Tyrosine-modified linear PEIs for highly efficacious and biocompatible siRNA delivery *in vitro* and *in vivo*.... *Nanomedicine: NBM* 2021;xx:-1-15, https://doi.org/10.1016/j.nano.2021.102403

nanomedicine
Nanotechnology, Biology, and Medicine

Highlights

Nanomedicine: Nanotechnology, Biology, and Medicine xxx (2021) xxx–xxx

Tyrosine-modified linear PEIs for highly efficacious and biocompatible siRNA delivery *in vitro* and *in vivo*

Michael Karimov[a], Marion Schulz[a], Tim Kahl[a], Sandra Noske[a], Malgorzata Kubczak[b], Ines Gockel[c], René Thieme[c], Thomas Büch[a], Anja Reinert[d], Maksim Ionov[b], Maria Bryszewska[b], Heike Franke[e], Ute Krügel[e], Alexander Ewe[a], Achim Aigner[a,*]

[a]*Rudolf-Boehm-Institute for Pharmacology and Toxicology, Clinical Pharmacology, Leipzig University, Faculty of Medicine, Leipzig, Germany*
[b]*Department of General Biophysics, University of Łódź, Łódź, Poland*
[c]*Department of Visceral, Transplant, Thoracic and Vascular Surgery, University Hospital Leipzig, Leipzig, Germany*
[d]*Faculty of Veterinary Medicine, Institute of Anatomy, Histology and Embryology, Leipzig University, Leipzig, Germany*
[e]*Rudolf-Boehm-Institute for Pharmacology and Toxicology, Leipzig University, Faculty of Medicine, Leipzig, Germany*

- Polyethylenimines (PEIs) are attractive systems for siRNA delivery *in vitro/in vivo*.
- Here, a set of small linear PEIs bearing tyrosine modifications (LP*x*Y) is explored.
- LP*x*Y show markedly enhanced transfection efficacy also in hard-to-transfect cells.
- LP*x*Y/siRNA complexes offer very favorable physical properties and biocompatibility.
- Nanoparticle efficacies are seen *in vitro*, *ex vivo* and in three tumor models *in vivo*.

Please cite this article as: Karimov M., et al., Tyrosine-modified linear PEIs for highly efficacious and biocompatible siRNA delivery *in vitro* and *in vivo*.... *Nanomedicine: NBM* 2021;xx:-1-14, https://doi.org/10.1016/j.nano.2021.102403

ELSEVIER
Nanomedicine: Nanotechnology, Biology, and Medicine
xx (xxxx) xxx
nanomedicine Nanotechnology, Biology, and Medicine
nanomedjournal.com

Tyrosine-modified linear PEIs for highly efficacious and biocompatible siRNA delivery *in vitro* and *in vivo*

Michael Karimov[a], Marion Schulz[a], Tim Kahl[a], Sandra Noske[a], Malgorzata Kubczak[b], Ines Gockel[c], René Thieme[c], Thomas Büch[a], Anja Reinert[d], Maksim Ionov[b], Maria Bryszewska[b], Heike Franke[e], Ute Krügel[e], Alexander Ewe[a,1], Achim Aigner[a,*,1]

[a]*Rudolf-Boehm-Institute for Pharmacology and Toxicology, Clinical Pharmacology, Leipzig University, Faculty of Medicine, Leipzig, Germany*
[b]*Department of General Biophysics, University of Łódź, Łódź, Poland*
[c]*Department of Visceral, Transplant, Thoracic and Vascular Surgery, University Hospital Leipzig, Leipzig, Germany*
[d]*Faculty of Veterinary Medicine, Institute of Anatomy, Histology and Embryology, Leipzig University, Leipzig, Germany*
[e]*Rudolf-Boehm-Institute for Pharmacology and Toxicology, Leipzig University, Faculty of Medicine, Leipzig, Germany*

Revised 28 March 2021

Abstract

Therapeutic gene silencing by RNA interference relies on the safe and efficient *in vivo* delivery of small interfering RNAs (siRNAs). Polyethylenimines are among the most studied cationic polymers for gene delivery. For several reasons including superior tolerability, small linear PEIs would be preferable over branched PEIs, but they show poor siRNA complexation. Their chemical modification for siRNA formulation has not been extensively explored so far. We generated a set of small linear PEIs bearing tyrosine modifications (LP*x*Y), leading to substantially enhanced siRNA delivery and knockdown efficacy *in vitro* in various cell lines, including hard-to-transfect cells. The tyrosine-modified linear 10 kDa PEI (LP10Y) is particularly powerful, associated with favorable physicochemical properties and very high biocompatibility. Systemically administered LP10Y/siRNA complexes reveal antitumor effects in mouse xenograft and patient-derived xenograft (PDX) models, and their direct application into the brain achieves therapeutic inhibition of orthotopic glioma xenografts. LP10Y is particularly interesting for therapeutic siRNA delivery.

Key words: Tyrosine-modified linear polyethlyenimines; siRNA transfection; Therapeutic siRNA delivery; RNAi *in vivo*; Tumor xenografts and PDX models

RNA interference (RNAi) is a powerful strategy for the treatment of various diseases, based on the target-specific silencing of pathologically over-expressed genes.[1] It is mediated by small interfering RNAs (siRNAs), allowing for the specific knockdown of any target gene of interest.[2,3] One of the great challenges is the safe and efficient delivery of siRNAs, especially for *in vivo* application based on systemic injection. Rapid enzymatic and non-enzymatic degradation, renal elimination, poor cellular uptake and insufficient intracellular release from the endo-/lysosomal compartment still pose major hurdles for siRNA therapies *in vivo* and for their translation into the clinic.[4,5]

Since viral delivery systems have several disadvantages, non-viral approaches have been extensively explored. These include chemical siRNA modification and the conjugation of siRNAs *e.g.* to GalNAc for targeted delivery to hepatocytes, as well as nanoparticle systems such as cationic liposomes, polymers or inorganic compounds (see *e.g.*[6,7]). Much attention has been focused on cationic polymers. Polyethylenimine (PEI) is one of the most studied polymers for gene delivery.[8,9] With a nitrogen atom at every third position, PEI has a high charge density allowing for nucleic acid complexation and condensation by electrostatic interactions, protection of the payload, as well as facilitated interaction with the cellular membrane. Linear or

Conflicts of interest: There are no conflicts to declare

* Corresponding author at: Rudolf-Boehm-Institute for Pharmacology and Toxicology, Clinical Pharmacology, Leipzig University, Leipzig, Germany.
E-mail address: achim.aigner@medizin.uni-leipzig.de. (A. Aigner).
[1] These senior authors contributed equally.

https://doi.org/10.1016/j.nano.2021.102403
1549-9634/

branched PEIs are commercially available over a broad range of molecular weights (0.8-200 kDa),[10] with toxicity, complexation efficacy and biological activity depending on the molecular weight. While high molecular weight PEIs show satisfying complexation efficacy, they are associated with higher toxicity. *Vice versa*, lower molecular weight PEIs provide better biocompatibility but unfavorable properties for gene transfer. This is particularly true for the delivery of small nucleic acids, such as siRNA.[11] While certain branched low-molecular weight PEIs have been found efficient for siRNA delivery, linear PEIs (LPEI) show higher biocompatibility[12] and may thus also show advantages upon chemical modification, but they are largely inactive due to poor siRNA complexation efficacy.[13]

The further investigation of linear PEIs (LPEIs) is also particularly interesting for other reasons. Synthesis conditions have been optimized towards allowing the manufacturing of linear PEIs with a narrow size distribution and less batch-to-batch variation. They thus differ from branched PEIs which have broader size distributions and vary in the stoichiometry of their 1°/2°/3° amine contents.[14,15] The precursor polymers for linear PEIs, polyoxazolines, are currently tested as non-immunogenic PEG alternatives in clinical trials.[16] Likewise, the 25 kDa linear PEI (known as *in vivo* jetPEI®) successfully entered clinical trials for the delivery of plasmid DNA (pDNA) for different medical applications,[17–19] and another study used a mannobiose-modified LPEI/pDNA complex for vaccination against HIV *via* the dermal route.[20] The current clinical developments, however, primarily focus on the delivery of large pDNA rather than small RNAs like siRNA or miRNA, mainly caused by the suboptimal ability of linear PEIs to complex and deliver small and rigid nucleic acids like small RNAs.[13] Current strategies to improve LPEI-mediated siRNA transfection rely on increasing the siRNA size by using "sticky siRNAs",[21–23] the combination of LPEI/siRNA complexes with liposomes ("lipopolyplexes"[24];) or the chemical modification of LPEIs. Examples include the cross-linking of LPEIs to branched molecules,[25] hexadecyl groups[26] or hydroxyethyl groups,[27] or the synthesis of PEI-PEG-PCL copolymers.[28]

Branched PEIs have been modified previously with different amino acids, leading to marked alterations in their properties.[29,30] The modification with aromatic amino acids phenylalanine, tryptophan and tyrosine has been shown to lead to improved biocompatibility and efficient siRNA delivery *in vitro* and identified the tyrosine derivative as most active.[31,32] A possible explanation for this efficacy might be improved proton sponge and polymer self-assembly properties.[33] Previously, we used a range of branched low molecular weight PEIs (2, 5 and 10 kDa) for tyrosine modification, and explored them *in vitro* and *in vivo*.[34,35] However, the use of linear (rather than branched) PEIs with low molecular weight would be more preferable for the reasons described above, but it has not been explored so far.

In this study, we generated a set of various linear polyethylenimines (2, 5, 10 and 25 kDa) bearing tyrosine modifications. From the assessment of these compounds for their capacity for siRNA delivery *in vitro* in various cancer cell lines, *ex vivo* in a tumor tissue slice model, and *in vivo* in complex tumor xenograft mouse models, we identify the tyrosine-derivative of linear 10 kDa PEI as particularly efficient. This is associated with favorable physicochemical properties and high biocompatibility, thus providing the basis for its possible translation into clinical studies.

Methods

Further information regarding materials and methods is given in the supplementary material.

Chemical synthesis of tyrosine-modified linear PEIs

Linear PEI (40 mg, 0.93 mmol in monomer units) was dissolved in 3 mL DMF, followed by addition of N,N-diisopropylethylamine (2 eq.; 325 µL, 1.86 mmol). N-Boc-tyrosine (0.5 eq.; 131 mg, 0.465 mmol) was dissolved in 2 mL DMF, added to the polymer solution and stirred for ~15 min, prior to the addition of benzotriazole-1-yl-oxy-tris-pyrrolidino-phosphonium hexafluorophosphate (PyBOP) (0.7 eq.; 520 mg, 0,651 mmol) and stirring at RT for 48 h. Afterwards, DMF and other low molecular weight impurities were removed by dialysis (MWCO 3.5 kDa, SpectraPor, Serva, Heidelberg, Germany) against methanol for 6 h. For deprotection, the methanolic polymer solution was mixed with the same amount of trifluoracetic acid (~3 mL each) and stirred overnight. Methanol was then removed *in vacuo*, while excess TFA was removed by co-evaporation with ethanol (3 × 25 mL). The product was dissolved in methanol and dialyzed against methanol (1 day), 0.1 M HCl in methanol (12 h), 0.1 M HCl in dH_2O (12 h) and distilled water (1.5 days). Finally, the product was lyophilized to obtain tyrosine-modified linear PEI as a white powder, and characterized by ^{1}H NMR (400 MHz, solvent: D_2O). The tyrosine content was determined according to the formula in Suppl. Figure 1. The tyrosine-modified LPEIs were abbreviated as follows: LP*x*Y with *x* = molecular weight of the LPEI.

Cell culture, complex preparation and transfection

All cell lines were cultivated under standard conditions (37 °C, 5% CO_2) in RPMI-1640 medium supplemented with 10% FCS. For transfection, cells were seeded into 24-well plates at 3.5×10^4 cells per well containing 0.5 mL medium, or at 1×10^3 cells/well in 100 µL medium (96 well plates). Unless stated otherwise, no further medium change was done before or after addition of complexes. LP*x*Y/siRNA complexes for one well (24-well plate) were prepared by mixing 0.4 µg (30 pmol) siRNA per well in 12.5 µL HN buffer (150 mM NaCl, 10 mM HEPES, pH 7.4) with 1 µg LP*x*Y in 12.5 µL HN buffer, prior to incubation for 30 min. For assessing the influence of FCS on the transfection efficacies, LP*x*Y/siRNA complexes were incubated in the presence of different FCS concentrations and under various conditions (1 h at RT, 3 days at 4 °C, 3 days at RT or 3 days at 37 °C).

Tissue slice preparation, cultivation, and treatment

Under sterile conditions, 350 µm thick tissue slices were prepared from HROC24 tumor xenografts using a Leica VT 1000 vibratome (Leica Microsystems, Wetzlar, Germany). Slices

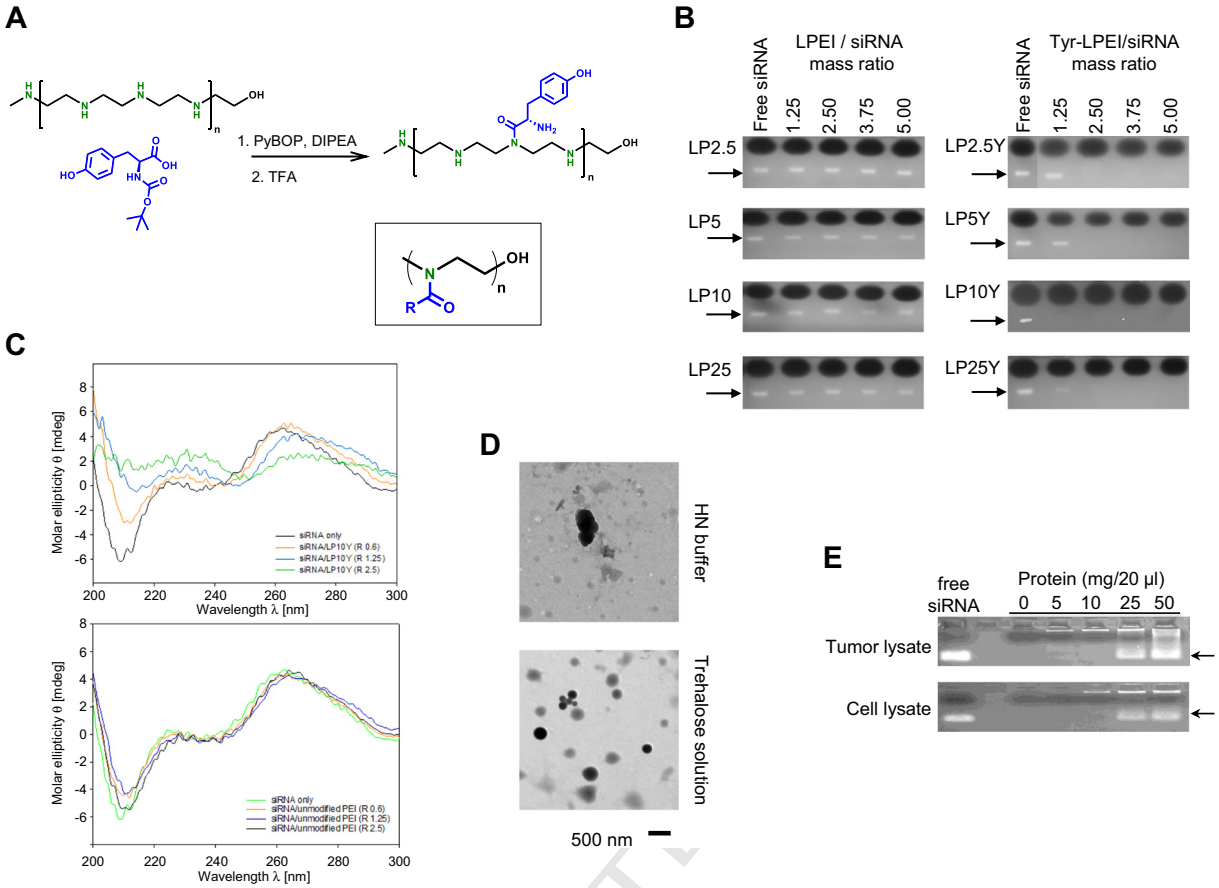

Figure 1. Chemical polymer synthesis and complex properties. **(A)** Synthesis scheme for tyrosine-modification of linear PEI; inset: structure similarity to poly(2-ethyl-2-oxazoline). **(B)** siRNA complexation efficacies of linear PEIs with molecular weights between 2.5 and 25 kDa (LP2.5-LP25; left) and their tyrosine-modified counterparts (right) at different polymer/siRNA mass ratios. Arrow: free siRNA. **(C)** CD spectrometry of LP10Y/siRNA (upper panel) and 10 kDa LPEI/siRNA mixtures (lower panel) with different polymer/siRNA mass ratios (see color code). Alterations of curves with increasing polymer/siRNA mass ratio indicate complex formation. **(D)** Transmission electron microscopic images of LP10Y/siRNA complexes, generated in HN buffer (upper images) or trehalose solution (lower images). **(E)** Assessment of complex stability in the presence of increasing concentrations of proteins derived from tumor xenograft (upper panel) or cell lysates (lower panel). Arrow: free siRNA.

were then stamped to a diameter of 3 mm (disposable biopsy punch 3 mm; pfm medical ag, Köln, Germany) and placed onto membrane culture inserts with a pore diameter of 0.4 µm (Sarstedt, Nümbrecht, Germany), in 6-well plates containing 1 mL RPMI-1640 (10% FCS, 1% penicillin/streptomycin). After incubation overnight (humidified atmosphere, 5% CO_2, 37 °C), the slices were transferred to a 96-well plate containing 100 µL pre-warmed medium. LP10Y/siRNA complexes were added to the slices and incubated for 6 h, prior to placing them back on the membrane culture inserts and further cultivation, with the medium being replaced every day. After 72 h incubation, slices were collected for further analysis by RT-qPCR and Western blotting (see Suppl. Materials and Methods for details).

In vivo therapy in subcutaneous and orthotopic xenografts

Athymic nude mice (Foxn1nu/nu; Charles River Laboratories, Sulzfeld, Germany) or SCID mice (NOD/SCID/IL2r gamma (null); Jackson Laboratories, Bar Harbor, ME) were kept at 25 °C in a humidified atmosphere, 12 h light/dark cycle, with species-specific food and water *ad libitum*. Animal studies were performed according to the national regulations and approved by the local authorities (Landesdirektion Sachsen). All animal experiments complied with the ARRIVE guidelines and were carried out in accordance with the EU Directive 2010/63/EU for animal experiments. For the generation of subcutaneous (s.c.) tumor xenografts, 5×10^6 HROC24 cells in 150 µL PBS were s.c. injected into both flanks of the mice. When xenografts reached a size of ~100 mm^3, mice were randomized into four different treatment groups (untreated, LP10Y-complexed siCTRL, siSurvivin, or siPLK; 6-9 tumors/group). Complexes were prepared as described above and amounts corresponding to 10 µg siRNA were i.p. injected 3 times a week over 2 weeks, with regular control of tumor size, animal behavior and body weight. After termination of the *in vivo* studies, mice were sacrificed by isoflurane overdosage and cervical dislocation, tumors and other organs were excised and snap-frozen or fixed in formalin for further analysis.

The patient-derived xenograft (PDX) model was derived from an adenocarcinoma of the esophagogastric junction (EGJ tumor

tissue). Of note, neoadjuvant chemotherapy according to the FLOT (5-FU/leucovorin/oxaliplatin/docetaxel) protocol had been administered before. Tumor specimens of 30 mm^3 were used for PDX generation. 30 min prior to implantation, SCID mice were given metamizol i.p., followed by isoflurane anesthesia. The tumor tissue was implanted into a s.c. pouch in the flank region of the mice, and the wound was closed using histoacryl tissue adhesive. Maximum delay between surgical removal of tumor tissue and primary engraftment of the mice was 4 h. In order to prevent wound infection, mice received 1.45 mg/ml cotrimoxazol p.o. *via* drinking water for 10 days after transplantation. PDX tumor tissues were propagated in mice for three rounds. Six weeks after tumor transplantation, treatment was performed 3 times a week by i.p. application of nanoparticles as described above. At the end of the experiment, tumor sizes were determined and organs (brain, lung, liver, kidney, bowel) as well as lymph nodes were removed, fixed and paraffin embedded.

For the generation of orthotopic glioblastoma xenografts, a guide-screw system (Plastics One, Roanoke, VA) was used to perform the intracerebral tumor cell engraftment and subsequent injections of LP10Y/siRNA complexes. Guide screw implantation was performed essentially as described previously.[36] Briefly, carprofen-pretreated mice were anesthetized by isoflurane, prior to making a ~1 cm incision the scalp and removing the underlying periosteum. After drilling a 1-mm burr hole into the skull 1 mm rostral and 2 mm lateral to the bregma, the guide screw was screwed into the burr hole. Two days after the implantation of guide screws, 3×10^5 G55T2 glioblastoma cells in 2 μL PBS were injected through the screw into the basal ganglia of the mice, using a 27-gauge needle attached to a 25-μL Hamilton syringe. Treatment was started at 7 days after tumor inoculation, with 3 injections (days 5, 7, 10) over one week (assessment of mouse survival) or with 6 injections over two weeks (glioma xenograft analysis). Mice were anesthetized as above prior to injecting 3 μL complexes containing 0.5 μg siRNA at a flow rate of 12 μL/h. Upon termination of the experiment 3 days after the last injection, mice were sacrificed as above and brains were fixed in 4% paraformaldehyde solution. For tumor size determination, vibratome sections were prepared and stained with cresyl violet. For immunohistochemistry, brains were fixed in formalin for paraffin-embedding.

In vivo biodistribution and analysis of adverse effects

For the determination of *in vivo* LP10Y/siRNA complex biodistribution, siRNA was radioactively labeled with γ-[32P]-ATP (Hartmann Analytic, Braunschweig, Germany), using the enzyme T4 polynucleotide kinase (Thermo Scientific) according to the manufacturer's protocol. Labeled siRNA was mixed with unlabeled siRNA at ratio of 1:4 and the complexes were prepared as described above and injected i.p. or i.v. into HROC24 tumor xenograft-bearing mice. After 4 h, mice were sacrificed and tissues were collected for RNA isolation. Tissue samples were weighted and homogenized in 1 mL TriFast reagent using an ULTRA-TURRAX® homogenizer (IKA, Staufen, Germany). Volumes containing more than 300 mg tissue were further diluted with TriFast up to 1 mL. RNA was extracted following the manufacturer's protocol, dissolved in 100 μL formamide and heated for 10 min at 80 °C. 40 μL sample was mixed with 10× loading dye and run on a 1% denaturing agarose gel (0.9% formaldehyde) with TAE running buffer. The RNA was transferred onto a Hybond-N+ membrane (Merck Millipore), using standard capillary blot techniques (20× SSC transfer buffer (3 M NaCl, 300 mM sodium citrate in DEPC-H_2O). Bands representing intact siRNA were visualized by autoradiography (Fuji BAS 1000, Fuji, Düsseldorf, Germany) and quantitated using free ImageJ software (NIH, Bethesda, MD).

The absence of immunostimulation of the LP10Y/siRNA complexes was tested using the analysis of the immunostimulatory cytokines (INF-γ, TNF-α). For this, LP10Y/siRNA complexes (10 μg siRNA) were i.v. injected twice within 24 h into immunocompetent C57BL/6 mice. Four hours after the last injection, the blood was collected for analysis. Mice treated with lipopolysaccharides (LPS) 50 μg in 150 μL (single injection) served as positive control and untreated mice served as negative control. The serum levels of INF-γ and TNF-α were determined using an ELISA kit (PreproTech, Hamburg, Germany) following the manufacturer's instructions. For monitoring effects on body weight, mice were 5× over 9 days treated by i.p. injection of complexes.

Statistics

Statistical analyses were performed by Student's *t* test or one-way ANOVA, and significance levels are * = $P < 0.03$, ** = $P < 0.01$, *** = $P < 0.001$. Unless indicated otherwise, differences between specific and non-specific treatment were analyzed, with at least $n = 3$.

Results

Preparation of tyrosine-modified LPEIs

Linear PEIs of different molecular weights between 2.5 and 25 kDa were grafted with activated tyrosine according to the scheme depicted in Figure 1, *A*. Initially, optimal reaction conditions for the tyrosine modification of LPEI had to be determined. Based on the previous results for the tyrosine-modified branched PEIs,[35] a 30% tyrosine grafting was attempted. However, using the same conditions with EDC/NHS as coupling reagents and DMF/DCM as solvent mixture failed, only leading to a tyrosine grafting of 3-5%. Increasing the reactant concentrations or switching to the coupling reagent DMTMM in water or water/methanol proved unsuccessful with regard to further increasing the tyrosine substitution grade as well. Only the more reactive coupling reagent PyBOP, in combination with dimethyl formamide (DMF) as solvent, finally yielded the desired tyrosine grafting rates. The successful tyrosine modification was confirmed by ^1H NMR (Suppl. Figure 1, *A*, Suppl. Table 4), with tyrosine contents between ~30 and 36% (Suppl. Figure 1, *B*).

Characterization of complexes based on tyrosine-modified LPEIs

This high degree of tyrosine modification led to polymers considerably different from the parent PEIs, in part resembling a poly(2-ethyl-2-oxazoline) structure (Figure 1, *A*, inset). Notably,

the linear tyrosine-modified PEIs (LP*x*Y; Linear PEI x kDa, tyrosine (Y) grafted) showed substantially enhanced complexation efficacies of siRNAs compared to the respective parent PEIs. More specifically, gel electrophoresis of complexation reactions at different polymer/siRNA mass ratios revealed essentially no siRNA complexation in the case of the unmodified PEIs, independent of their molecular weight (Figure 1, *B*, left). In contrast, the tyrosine-modified PEIs were able to mediate full siRNA complexation already at mass ratio 2.5 (Figure 1, *B*, right; note the absence of the free siRNA band). This complex formation was found for tyrosine-modified PEI with molecular weight as low as 2.5 kDa. LP10Y was identified as even more efficient, with full complexation already at mass ratio 1.25, while the even higher molecular weight of LP25Y did not further contribute to complexation efficacy. LP10Y was thus selected for further studies. LP10Y-mediated complexation at mass ratios 1.25-2.5 was also confirmed by CD spectrometry, while again no complex formation was observed in the case of its unmodified 10 kDa PEI counterpart (Figure 1, *C*, upper *vs.* lower panel). LP10Y/siRNA complex sizes were dependent on buffer conditions during complexation and increased from ~135 nm in 20 mM HEPES/ 10% trehalose buffer to ~300 nm when using 10 mM HEPES/ 150 mM NaCl buffer (HN buffer; Table 1). Still, these LP10Y/ siRNA complexes were smaller than their counterparts based on LP2.5Y, LP5Y or LP25Y, where very large complexes of up to 750 nm were found in HN buffer. Independent of complex sizes, zeta potentials were always determined in the range of ~10.5-23.5 mV in the HEPES/trehalose buffer and 2.1-10.5 mV in HN buffer, respectively (Table 1). Complex sizes were also confirmed by transmission electron microscopy, showing distinct round-shaped nanoparticles prepared from the HEPES/ trehalose buffer and larger, less homogenous and spherical complexes formed in HN buffer (Figure 1, *D*). Complexes prepared in HN buffer were found to be more efficient for cell transfection in 2D cell culture as compared to their counterparts prepared in trehalose buffer (>90% *vs.* ~66% knockdown efficacy; data not shown). Thus, for subsequent *in vitro* experiments HN buffer was used for complexation.

Table 1
Sizes and zeta potentials of LP*x*Y/siRNA complexes.

Polymer	Buffer	Size [nm] (PDI)	Zeta potential [mV]
	10 mM HEPES 150 mM NaCl	564.45 ± 34.51 (0.353)	10.44 ± 0.44
LP2.5Y	20 mM HEPES 10% Trehalose	159.2 ± 0.7 (0.294)	21.36 ± 0.94
	10 mM HEPES 150 mM NaCl	759.83 ± 25.02 (0.321)	7.48 ± 2.38
LP5Y	20 mM HEPES 10% Trehalose	139.2 ± 2.7 (0.632)	10.53 ± 1.11
	10 mM HEPES 150 mM NaCl	304.03 ± 32.32 (0.218)	2.13 ± 0.08
LP10Y	20 mM HEPES 10% Trehalose	134.6 ± 1.1 (0.252)	23.58 ± 2.98
	10 mM HEPES 150 mM NaCl	628.66 ± 68.91 (0.244)	8.34 ± 6.93
LP25Y	20 mM HEPES 10% Trehalose	333.6 ± 2.8 (0.378)	14.02 ± 1.84

Biological properties and activities of LP10Y/siRNA complexes

Even at LP10Y/siRNA mass ratio as low as 2.5, complexes were found very stable, fully resistant to dissociation in the presence of high-dose heparin (Suppl. Figure 2, *A*, left). Complex stabilities were not impaired by addition of 50% FCS prior to heparin incubation (Suppl. Figure 2, *A*, right). Since this could indicate insufficient intracellular siRNA release from the complexes, experiments were repeated with increasing concentrations of a total tissue lysate (prepared from a tumor xenograft) or cell lysate. Under both conditions, which resemble more closely a biological situation in cells, partial complex decomposition was observed starting at 25 mg protein/20 μL solution (Figure 1, *E*), thus confirming the possibility of siRNA release from the complex upon cellular internalization.

The time-dependent microscopic analysis after transfection of H441 cells with LP10Y-complexed, Atto488-labeled siRNA revealed rapid complex uptake, beginning at 30-60 min after transfection start with continuous increase over 6 h (Suppl. Figure 2, *B*). Concomitantly, membrane fluidity analyzed by fluorescence anisotropy with 1,6-diphenylhexatriene (DPH) or its trimethylammonium derivative (TMA-DPH) as extrinsic membrane probes revealed the concentration dependent interaction of LP10Y. This was considerably more profound than in the case of its non-tyrosine modified counterpart LP10 (Suppl. Figure 2, *C*). In agreement with this, LP10Y/siRNA complex uptake efficacies were determined to be considerably more profound as compared to their counterparts without tyrosine modification. Indeed, flow cytometry revealed >10-fold higher intracellular levels of fluorophore-labeled siRNAs in H441 cells upon transfection with LP10Y/siRNA complexes (Suppl. Figure 3, *A* ± *B*). This was also confirmed by confocal microsopy, where cells were transfected with LP10Y complexed, Alexa647-labeled siRNA and the lysosomes were stained with Lysotracker green. After 24 h, complex uptake was observed in the majority of cells, with signals being mostly colocalized with Lysotracker signals and thus appearing as yellow, indicating subcellular localization in the lysosomes. However, many cells also showed strong red fluorescence, scattered or diffuse throughout the cytoplasm, indicating released siRNA (Suppl. Figure 3, *C*). In contrast, no detectable uptake was seen in the case of the LP10/siRNA complexes (Suppl. Figure 3, *D*).

The combination of improved complexation efficacy, enhanced membrane interaction and high complex stability of tyrosine-modified PEIs led to substantially increased siRNA-mediated knockdown efficacies and improved biocompatibility. Independent of molecular weights between 2.5 and 25 kDa, an at least 80-90% reduction of luciferase activity over the corresponding negative control was observed in H441-luc reporter cells without adverse effects on cell viability. In contrast, their non-modified counterparts were largely inactive and, with increasing molecular weight, rather toxic (Figure 2, *A*). This was particularly true for the 10 kDa linear PEI (LP10), which benefitted most from tyrosine grafting. This improvement of its biological activity and biocompatibility was strongly dependent on the degree of tyrosine grafting, with ~30% tyrosine content identified as optimal while lower degrees of modification with tyrosine were found insufficient and higher tyrosine content

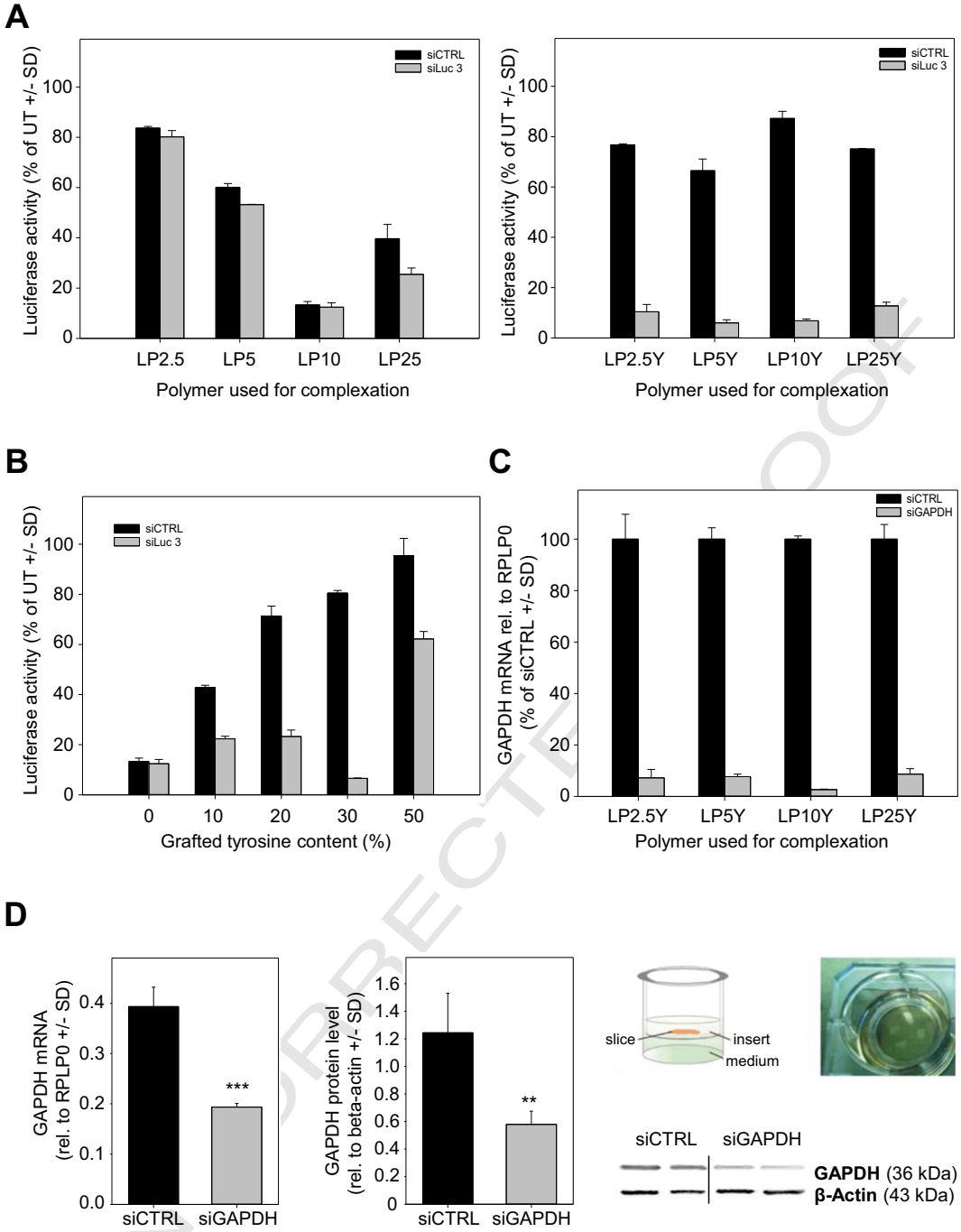

Figure 2. Biological knockdown efficacies *in vitro* and *ex vivo*. **(A)** Knockdown efficacies of complexes based on linear PEIs with molecular weights between 2.5 and 25 kDa (LP2.5-LP25; left) and their tyrosine-modified counterparts (right) in H441-luc cells, as determined by luciferase reporter activities. Black and gray bars: complexes containing non-specific and luciferase-specific siRNAs, respectively. **(B)** Dependence of LP10Y/siRNA knockdown efficacies on the degree of tyrosine grafting. **(C)** Knockdown of an endogenous gene (GAPDH), as determined by RT-qPCR (RPLP0: loading control). **(D)** Analysis of knockdown efficacy in a tissue slice model. 350 µm tissue slices from HROC24 xenografts were cultivated in an air–liquid interface culture (scheme, upper right) and treated with LP10Y/siRNA complexes. Bar diagrams specific knockdown of GAPDH on the mRNA (left) and protein level (center). Lower right: original Western blot.

again impaired knockdown efficacy (Figure 2, *B*). Switching to an endogenous target gene (GAPDH), LP10Y was again identified as most efficient, mediating a >95% gene knockdown (Figure 2, *C*). This was also confirmed when reducing siRNA amounts employed for gene knockdown. Results on mRNA knockdown were paralleled by a concomitant reduction of luciferase protein levels (Suppl. Figure 4, *A*). In agreement with our results on complexation efficacy, a polymer/siRNA mass ratio of 2.5 was sufficient for exerting maximum knockdown effects, while a further increase of

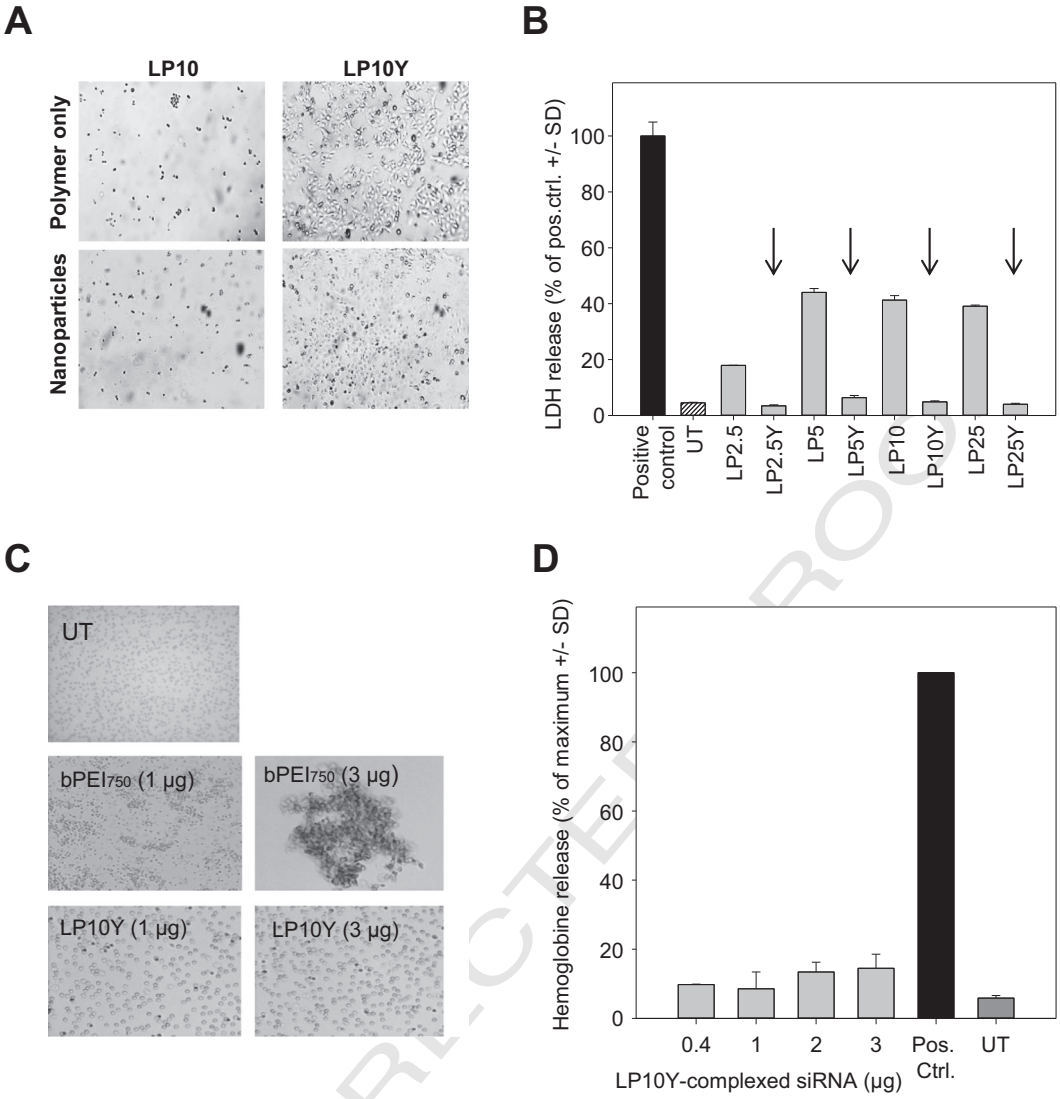

Figure 3. Analysis of LP10Y/siRNA biocompatibility. **(A)** Microscopic images of H441-luc cells 3 days after treatment with 10 kDa PEI or its tyrosine-modified derivative (upper panel), or the respective siRNA complexes derived thereof (lower panel). **(B)** LDH release assay for the assessment of cytotoxicity. H441-luc cells were transfected with complexes based on the various polymers and LDH levels were measured in the supernatant. Black bar: positive control (100% release); UT: untreated cells; arrows: complexes based onto tyrosine-modified PEIs. **(C)** Microscopic pictures from an erythrocyte aggregation assay after treatment with complexes as indicated. **(D)** Hemoglobin release from erythrocytes after treatment with LP10Y/siRNA complexes at various amounts. Black bar: positive control; UT: background level of untreated erythrocytes.

polymer content only led to cytotoxic effects without further improvement of knockdown (Suppl. Figure 4, *B*). This trend of LP10Y being most efficient was also observed in other cell lines (Suppl. Figure 5, *A*). Notably, beyond SKOV3 ovarian carcinoma cells this also covered rather hard-to-transfect cell lines like HCT116 colon carcinoma or HROC24 primary colon carcinoma cells, where still >70% knockdown was obtained (Suppl. Figure 5, *A*). In agreement with rapid complex uptake (see Suppl. Figure 2, *B*), maximum knockdown was achieved after 2-3 days (Suppl. Figure 5, *B*). Despite cell proliferation presumably leading to siRNA dilution, full knockdown efficacy was maintained at least until day 7, with an only slight decrease thereafter (day 10; Suppl. Figure 5, *B*, left). This indicates a rather rapid onset and long duration of target gene knockdown.

Studies were also extended towards *ex vivo* 3D tissue slice models, representing intact tumor tissue. For this, 350 µm slice from HROC24 tumor xenografts was cultivated in an air–liquid interface setting (see scheme in Figure 2, *D*, upper right) and treated once with LP10Y/siRNA complexes. Despite the intact tissue representing a permeation barrier, a >50% target gene knockdown was observed on the mRNA as well as on the protein level (Figure 2, *D*, left and center).

High biocompatibility of LP10Y/siRNA complexes

In addition to optimal knockdown activity, high biocompatibility and absence of adverse effects are critical requirements for nanoparticles identified as optimal for potential therapeutic use. The microscopic evaluation of cell density and viability upon

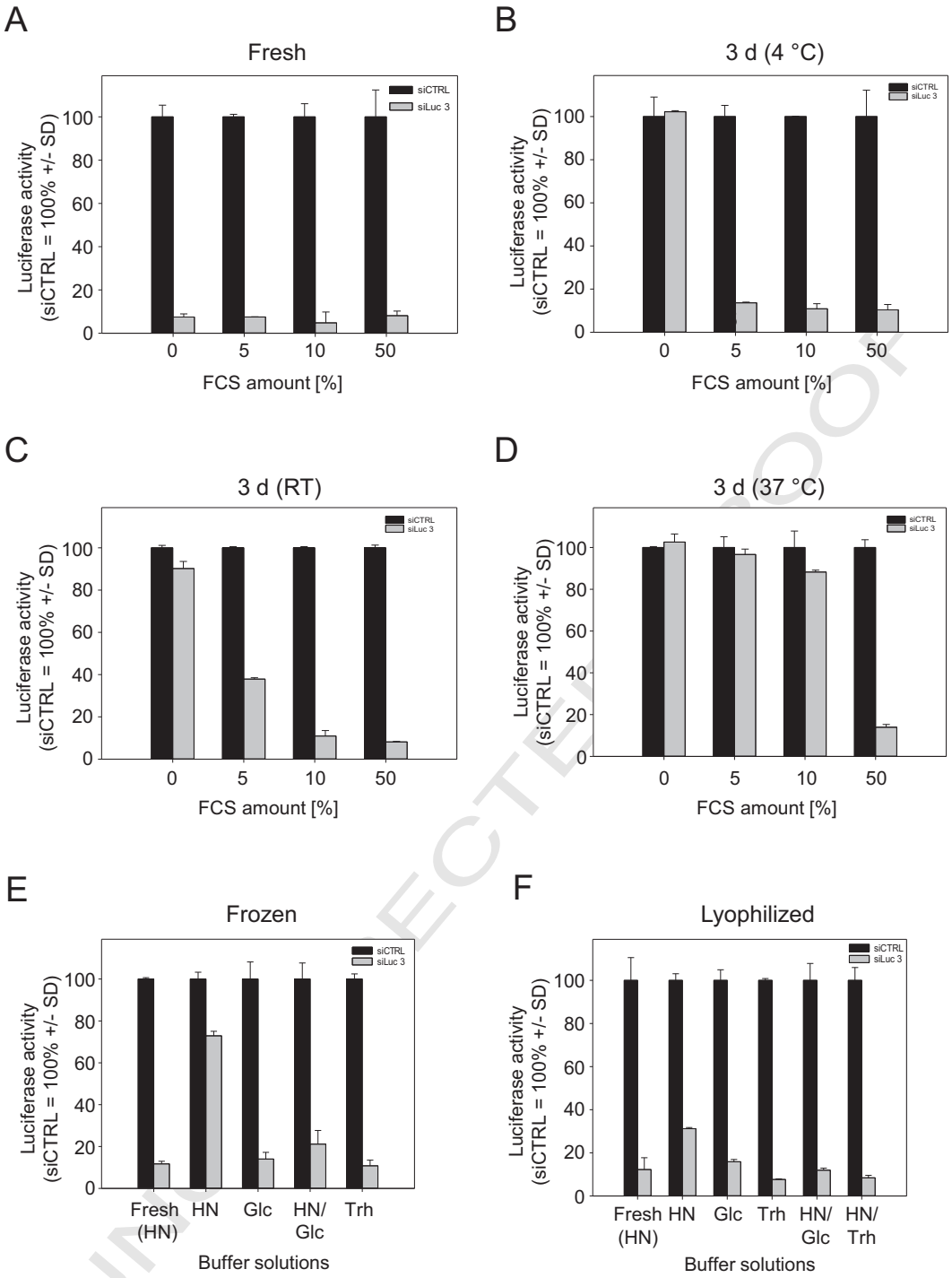

Figure 4. Biological knockdown efficacies of LP10Y/siRNA complexes in H441-luc cells under different conditions. **(A)** Knockdown efficacy upon pre-incubation of complexes in the presence of different concentrations of fetal calf serum (FCS). Black and gray bars: complexes containing non-specific and luciferase-specific siRNAs, respectively. Knockdown efficacies of complexes after incubation for 3 days at 4 °C **(B)**, at room temperature **(C)** or at 37 °C **(D)**. Knockdown efficacies of complexes prepared in different buffer solutions with subsequent storage at −20 °C (frozen; **E)** or lyophilization **(F)**.

treatment with nanoparticles or the corresponding free polymer revealed the above-noted enhancement of biocompatibility upon tyrosine-modification of linear PEI (Figure 3, *A*). This corresponded well with results from LDH release assays: independent of their molecular weight, toxicities of tyrosine-modified linear PEIs remained at background levels while their non-modified counterparts showed rather profound ~20% (2.5 kDa)-~40% (5 kDa and above) toxicity (Figure 3, *B*). Very good biocompatibility was also seen in erythrocyte aggregation and hemoglobin release assays, revealing no stimulation of

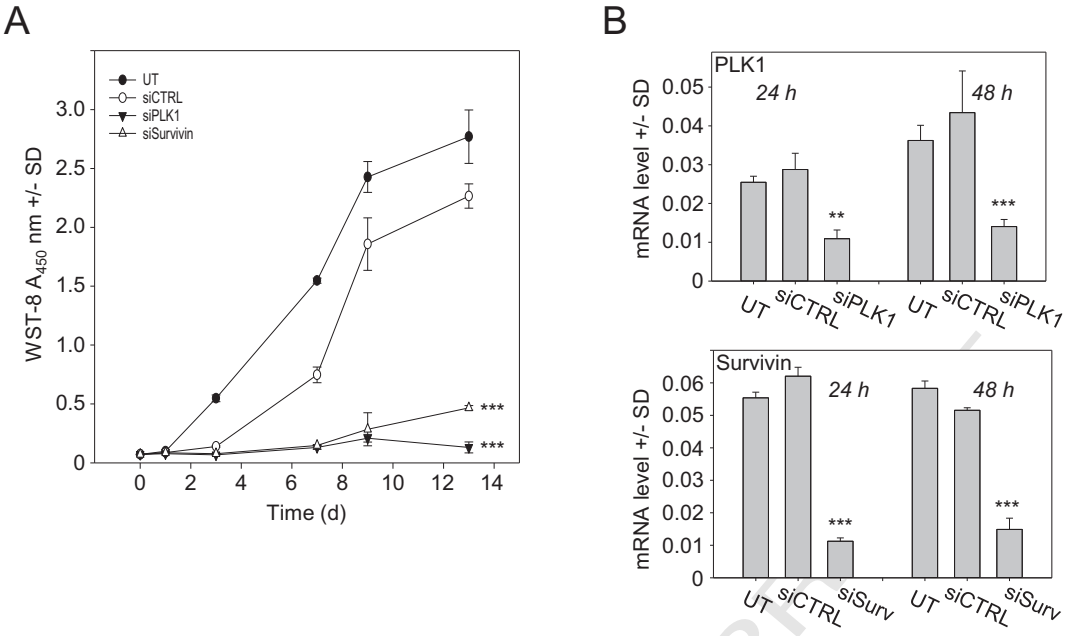

Figure 5. Tumor cell inhibition upon knockdown of oncogenes. **(A)** Proliferation assay of HROC24 cells upon transfection with LP10Y/siRNA complexes as indicated by the symbols. UT: untreated. **(B)** Tumor cell inhibition is based on the specific LP10Y/siRNA-mediated knockdown of PLK1 (upper panel) or Survivin (lower panel).

erythrocyte aggregation (Figure 3, *C*) and hemoglobin release only slightly above background (Figure 3, *D*). Absence of toxic effects was also confirmed in Caspase-3/-7 assays. No increase in Caspase-3/-7 activity was observed, excluding the induction of extrinsic or intrinsic apoptosis at 24 h or 72 h after transfection with LP5Y/siRNA or LP10Y/siRNA complexes (Suppl. Figure 6, *A*). This was accompanied by the absence of genotoxicity. In contrast to the positive control (H_2O_2), COMET assays revealed no genotoxic effects of LP10Y/siRNA complexes at 24 h after transfection into H441 cells (Suppl. Figure 6, *B*). This was also true for complexes based on the other tyrosine-modified linear PEIs (data not shown), while the non-modified counterpart of LP10Y, the 10 kDa linear PEI, showed dose-dependently single COMET signals at 30 pmol, indicating slight genotoxicity (Suppl. Figure 6, *B*; see quantitation and arrow in the right panel).

Analysis of cellular uptake properties and complex stability

For successful transfection, nanoparticle uptake is a major issue and was thus analyzed in greater detail. In agreement with the microscopic evaluation of cell uptake of LP10Y-complexed fluorophore-labeled siRNA (see Suppl. Figure 2, *B*), time-dependent medium exchange experiments revealed that >50% knockdown was already achieved when removing the complexes as early as 1 h after transfection and maximum knockdown efficacy was obtained upon incubation for ~6 h, with no further improvement thereafter (Suppl. Figure 7, *A*). To elucidate the mechanism of cell uptake of LP10Y/siRNA complexes, H441-luc cells were transfected in the absence/presence of various inhibitors (Suppl. Figure 7, *B*). The addition of DMSO as solvent control for the inhibitors exerted a minimal non-specific decrease in knockdown efficacy. In contrast, increasing concentrations of methyl-β-cyclodextrin (MBCD) as a widely used method for inducing acute depletion of cholesterol, which is essential for the formation of lipid rafts in cell membranes,[37] led to a dose-dependent reduction of luciferase knockdown. To the contrary, filipin-3 as inhibitor of caveolin-mediated internalization left bioactivities of LP10Y/siRNA complexes largely unchanged as compared to negative control treatment (DMSO), and in the case of chlorpromazine as inhibitor of clathrin-dependent internalization, high concentrations were required for some minor inhibition. Full abrogation of knockdown efficacy was seen under bafilomycine A1 treatment, an inhibitor of vacuolar ATPases that prevents endosome acidification, at already low concentrations (Suppl. Figure 7, *B*).

To address if these differential effects of inhibitors on knockdown efficacies are based on complex uptake or intracellular processing, experiments were extended towards monitoring LP10Y-complexed, fluorophore-labeled siRNA uptake. In agreement with knockdown data, methyl-β-cyclodextrin led to a dose-dependent decrease in cellular complex uptake (Suppl. Figure 7, *C*). This inhibition of complex uptake, however, was more pronounced than the decrease in knockdown efficacy (compare to Suppl. Figure 7, *B*), indicating that somewhat lower intracellular siRNA levels are still sufficient for inducing RNAi. This was also true for chlorpromazine where the dose-dependent inhibition of complex uptake was more profound than effects on knockdown, with the latter only seen at the highest inhibitor concentration. In line with the absence of filipin-3 effects on biological activity, no changes in complex uptake were observed. Taken together, this indicates that complex uptake is one major determinant of LP10Y/siRNA knockdown activity. In contrast, bafilomycin A1 did not impair complex uptake, albeit abolishing knockdown, thus identifying

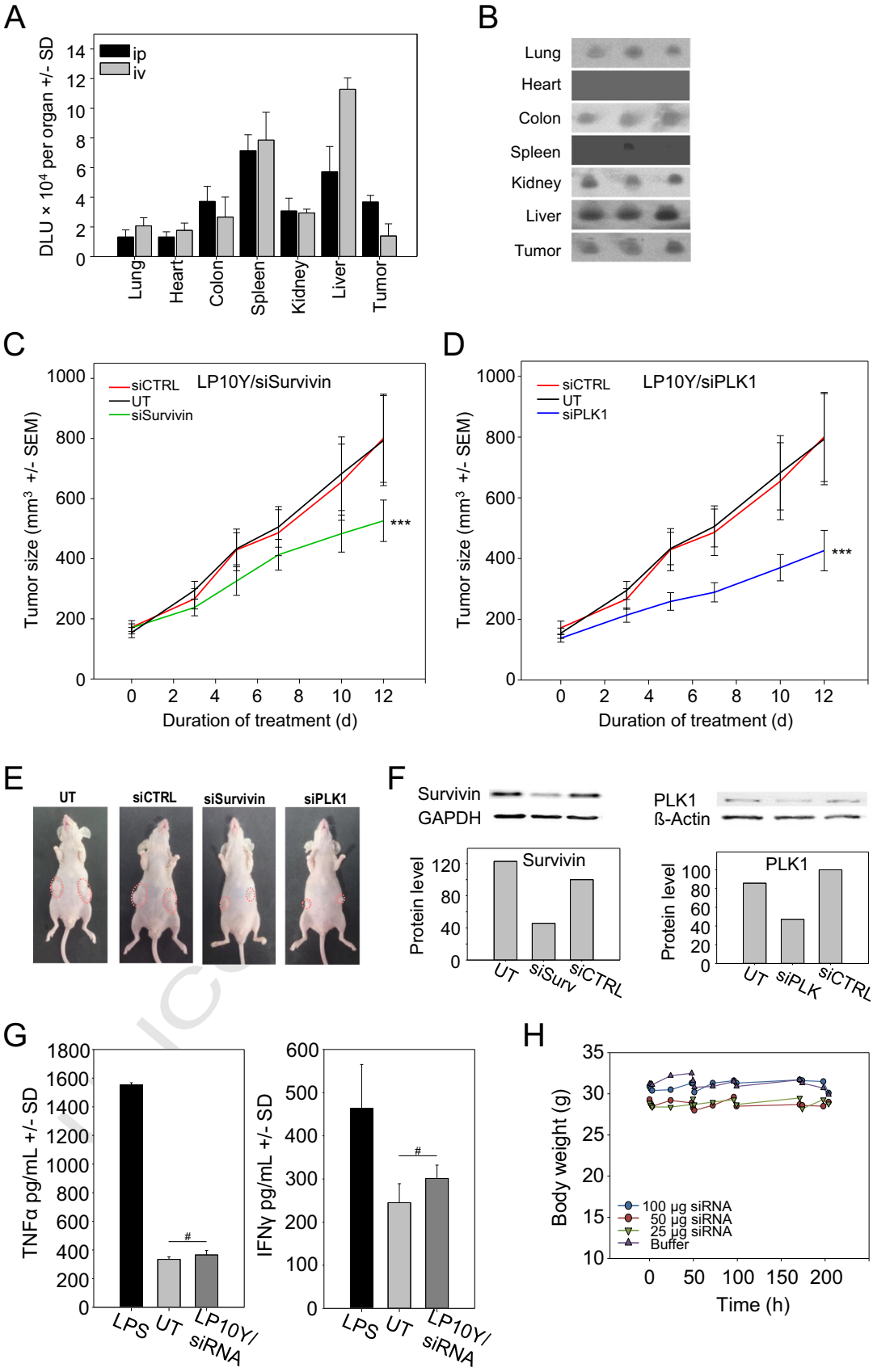
A
DLU × 10⁴ per organ +/- SD
ip
iv
Lung
Heart
Colon
Spleen
Kidney
Liver
Tumor
B
Lung
Heart
Colon
Spleen
Kidney
Liver
Tumor
C
LP10Y/siSurvivin
siCTRL
UT
siSurvivin
Tumor size (mm³ +/- SEM)
Duration of treatment (d)
***
D
LP10Y/siPLK1
siCTRL
UT
siPLK1
Tumor size (mm³ +/- SEM)
Duration of treatment (d)
***
E
UT
siCTRL
siSurvivin
siPLK1
F
Survivin
GAPDH
PLK1
ß-Actin
Protein level
Survivin
UT
siSurv
siCTRL
Protein level
PLK1
UT
siPLK
siCTRL
G
TNFα pg/mL +/- SD
LPS
UT
LP10Y/ siRNA
IFNγ pg/mL +/- SD
LPS
UT
LP10Y/ siRNA
H
Body weight (g)
100 µg siRNA
50 µg siRNA
25 µg siRNA
Buffer
Time (h)

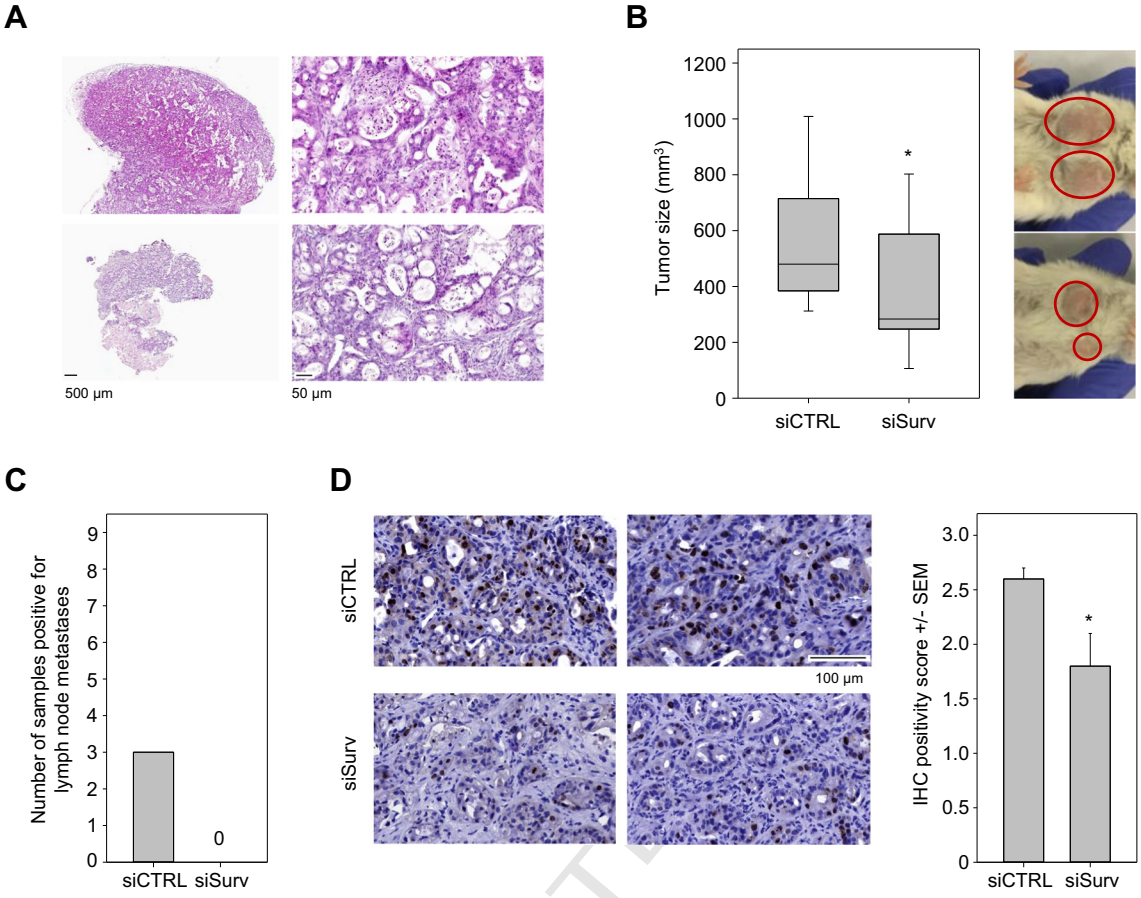

Figure 7. Therapeutic effects of LP10Y/siRNA complexes targeting Survivin in an s.c. PDX model. **(A)** Microscopic pictures showing the histology of a PDX tumor (upper panel) and a lymph node metastasis (lower panel). **(B)** Tumor-inhibitory effect of LP10Y/siSurv treatment, as determined at 12 weeks after treatment start. **(C)** Number of samples positive for lymph node metastases upon termination of the experiment. **(D)** Immunohistochemistry for Survivin (brown staining). Left: representative pictures of PDX tumors from negative control (upper panel) and specific treatment group (lower panel). Right: Quantitation of immunopositivity scores.

intracellular processing as critically involved in biological activity, besides cellular internalization.

For potential therapeutic use, stabilities of the complexes in the presence biological media and upon storage are critical parameters as well. Pre-incubation of LP10Y/siRNA complexes in the presence of up to 50% fetal calf serum (FCS) prior to transfection did not lead to alterations in knockdown efficacy, indicating full stability of the complexes towards high protein/serum concentrations (Figure 4, *A*). Quite in contrast, the addition of FCS was even found to fully protect complex activity during prolonged (3 days) storage at 4 °C, presumably by avoiding aggregation (Figure 4, *B*). For this, the addition of 5% FCS was already sufficient. Switching to higher temperatures, however, required higher FCS concentrations for protecting the complexes (Figure 4, *C*). Still, 10% FCS was sufficient at room temperature for the complete preservation of complex bioactivity over at least 3 days, and 50% FCS protected the complexes even at 37 °C (Figure 4, *D*). These findings regarding the FCS-mediated inhibition of complex aggregation were also confirmed by results from count rates in zetasizer measurements, which remained high upon storage, in particular at RT and 37 °C, only in the presence of serum (data not shown).

Next, the suitability of different storage forms was assessed. Freezing of the complexes protected their activity dependent on the buffer solution employed for complexation. Low ionic strength buffers containing glucose or trehalose as cryoprotectors

Figure 6. *In vivo* application of LP10Y/siRNA complexes in an s.c. tumor xenograft mouse model. **(A)** Radioactive biodistribution experiment, with bars indicating siRNA levels in the various organs at 4 h after i.p. (black) or i.v. injection (gray) of the complexes containing [32P]-labeled siRNA (DLU: density light units). **(B)** Autoradiography results from three mice after i.p. injection of the complexes. **(C, D)** Growth curves of HROC24 tumor xenografts upon treatment of mice as indicated in the figure (UT: untreated tumor-bearing mice). Tumor-inhibitory effects are observed in the specific treatment groups (LP10Y/siSurvivin **(C)** and LP10Y/siPLK1 **(D)**) *vs.* negative control groups (LP10Y/siCTRL and untreated). **(E)** Representative pictures of one mouse per group. **(F)** Knockdown of the respective target genes, Survivin (left) and PLK1 (right), as determined by Western blotting. **(G)** TNFα and IFNγ levels in immunocompetent mice treated by i.v. injection of LP10Y/siRNA complexes *vs.* negative control (untreated; UT). Black bar: positive control (lipopolysaccharide, LPS). **(H)** Monitoring of mouse body weights upon repeated i.p. application of LP10Y/siRNA complexes at different amounts.

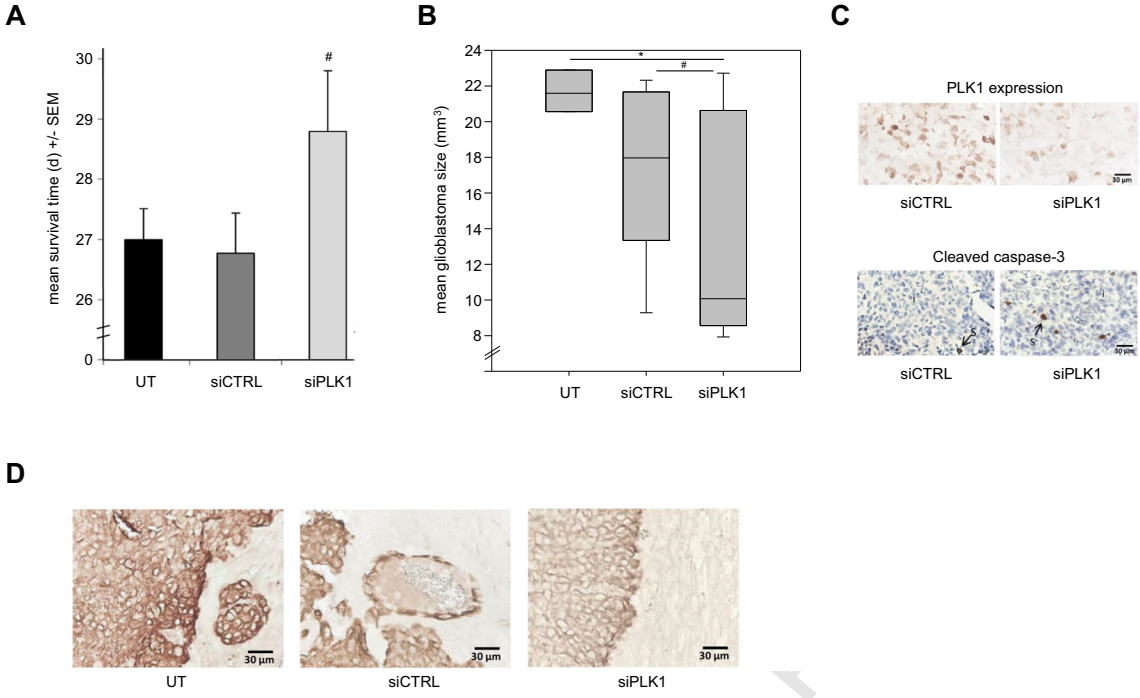

Figure 8. Therapeutic efficacy of LP10Y/siRNA complexes targeting PLK1 in an orthotopic glioblastoma mouse model. **(A)** Increase in mouse survival time upon treatment with LP10Y/siPLK1 complexes, as compared to negative control groups. UT: untreated tumor-bearing mice; #, n.s. **(B)** Decrease in mean glioblastoma sizes upon termination of the experiment. **(C)** Specific reduction of PLK1 expression levels (upper panel) and increase of cleaved Caspase-3 positive cells (lower panel) in the LP10Y/siPLK1 treatment group, as determined by immunohistochemistry. Bar: 10 µm. **(D)** Higher magnification of the edges of the tumors, immunohistochemically stained for Vimentin. Bar: 30 µm.

fully preserved knockdown efficacy, while using HEPES/NaCl buffer led to a profound reduction of the biological activity of frozen complexes (Figure 4, *E*). More importantly, complexes were found to be stable towards lyophilization. With the exception of complexes in HEPES/NaCl buffer where a slight reduction of knockdown efficacy was observed, complex activity was fully preserved (Figure 4, *F*).

Tumor cell-inhibitory effects of LP10Y/siPLK1 and LP10Y/siSurvivin complexes in vitro

Switching towards tumor-relevant oncogenes, Polo-like kinase 1 (PLK1) and Survivin, LP10Y/siRNA-mediated knockdown led to profound tumor cell inhibition, as demonstrated in HROC24 proliferation assays (Figure 5, *A*). While only slight non-specific transfection effects were observed when comparing growth curves of untreated and negative control LP10Y/siCtrl treated cells, transfection with LP10Y/siPLK1 or LP10Y/siSurvivin led to an essentially complete abolishment of tumor cell proliferation. RT-qPCR revealed that this was based on a profound knockdown of target gene mRNA levels, which, in particular in the case of Survivin, was fully established already at 24 h after transfection (Figure 5, *B*).

In vivo biodistribution and biocompatibility; efficacy in subcutaneous tumor xenografts

Most important is the usability of a nanoparticle system for therapeutic *in vivo* use. Preclinical therapeutic efficacy was initially assessed in s.c. tumor xenograft-bearing mice. Biodistribution of siRNA upon systemic application and in particular the delivery of intact full-length siRNA to its intended site of action were analyzed in a biodistribution assay based on radioactively labeled siRNA. 4 h after i.p. or i.v. application of LP10Y-complexed, [32P] end-labeled siRNA, various organs and tissues were taken, RNA was prepared and analyzed by gel electrophoresis and autoradiography. The delivery of intact, full-length siRNA is thus indicated by bands. Upon i.v. injection, major signals were detected in liver and spleen, as to be expected while delivery to other organs/tissues including tumor xenografts was low (Figure 6, *A*, Suppl. Figure 8, *A*). In contrast, i.p. administration of the LP10Y/siRNA complexes led to higher levels in the tumors, almost in the range of the liver (Figure 6, *A*, *B*). This indicated that the complexes become systemically available also after i.p. injection, and consequently delivery to other organs was observed as well. Based on these data, i.p. injection was chosen for subsequent therapy studies.

Upon establishment of s.c. HROC24 xenograft tumors with mean sizes of ~150-170 mm^3 and solid growth, mice were randomized into negative control (untreated, LP10Y/siCTRL) and specific treatment groups. Systemic treatment with LP10Y/siSurv complexes led to a ~40% reduction in tumor growth over 12 days (Figure 6, *C*). In the case of LP10Y/siPLK1 treatment, a more profound ~50% tumor inhibition was observed (Figure 6, *D*; see Figure 6, *E* for representative pictures of mice). Upon termination of the experiment, tumors were excised and analyzed for target gene expression. In both cases, analysis of tumor

lysates by Western blot revealed a >50% reduction of the target genes on the protein level (Figure 6, *F*). This finding also highlights, however, that a quite substantial inhibition of a single target gene may not be sufficient for therapeutic tumor control.

In vivo biocompatibility of LP10Y/siRNA complexes was assessed as well. Different tissues from the mice of the above therapy study were microscopically analyzed for histological alterations. Liver, lung, spleen and kidney did not reveal any differences between untreated and LP10Y/siRNA treated mice (Suppl. Figure 9). Furthermore, the complexes did not elicit an immune response. For this experiment, immunocompetent mice were chosen and no increases in TNFα or INFγ levels were observed even after i.v. injection of complexes (Figure 6, *G*). Likewise, no alterations in body weight were observed upon repetitive i.p. treatment over 9 days. This was also true for 10-fold higher LP10Y/siRNA amounts, corresponding to 100 μg siRNA (Figure 6, *H*).

Target gene knockdown and anti-metastatic effects in a patient-derived xenograft (PDX) model

Patient-derived xenografts represent the closest correlate to an original patient tumor, and are thus an ideal model for studying therapeutic effects. PDX from an adenocarcinoma of the esophagogastric junction was established in mice and propagated over three passages. The microscopic evaluation revealed a medium-grade differentiated adenocarcinoma with a Barrett's metaplasia (adenocarcinoma of the esophago-gastric junction (AEG) type I-II according to Siewert's classification), with the morphology and the distinct histological patterns of the initial tumor being well preserved (Figure 7, *A*, upper panel). These structures distinguished the PDX model from xenografts based on s.c. injected suspensions of tumor cell lines, as well as slower growth rates which thus resembled more the clinical situation. Notably, in untreated mice, lymph metastases were seen at the time point of termination of the experiment. More specifically, metastasis-positive lymph nodes appeared unstructured, with massive tumor infiltration (Figure 7, *A*, lower panel).

PDX-bearing mice were randomized when the tumors reached ~50 mm^3 and i.p. treated 3×/week over a period of 12 weeks with LP10Y/siSurv or LP10Y/siCTRL complexes. Upon termination of the experiment, the specific treatment group revealed a significant reduction in tumor size compared to negative control (Figure 7, *B*). Notably, metastasis formation was seen in 3/9 mice in the negative control group, while no metastases were observed in the specific treatment group (Figure 7, *C*). The microscopic analysis of paraffin sections of the tumors revealed that this tumor inhibitory effect was accompanied by a knockdown of the target gene, Survivin, as determined by immunohistochemistry (Figure 7, *D*).

Antitumor effects of LP10Y/siPLK complexes in an orthotopic glioma model

Finally, we also explored our P10Y/siRNA complexes for glioma treatment. For this, an orthotopic glioma xenograft model was used, which resembles more closely the *in vivo* situation than s.c. tumor xenografts. For the establishment and repeated treatment of orthotopic gliomas, a guide screw was implanted in the skull of immunodeficient mice three days prior to tumor cell injection. Pre-experiments revealed tumors at the earliest time point of analysis (6 days after injection of G55T2 cells), with moderate growth kinetics until day 14 (2.6-fold increase) and a rapid 10-fold increase in tumor size thereafter (day 14-25; data not shown). For the evaluation of specific PLK1 knockdown treatment effects on survival times upon, mice were injected three times (days 5, 7 and 10) with 3 μL LP10Y/siPLK complexes containing 0.5 μg siRNA. In order to avoid the blood–brain barrier, direct injection into the brain was performed, as described previously even in clinical studies.[38] The specific treatment led to an increase in overall survival time as compared to negative controls (Figure 8, *A*). Notably, no difference was observed between untreated and LP10Y/siCTRL treated mice, indicating the absence of non-specific toxicity of the complexes even upon direct complex injection into the brain.

For further analysis of the treatment effects on the glioma xenografts, the experiment was repeated with treatment six times every 2-3 days in the period of days 7-18, prior to explantation of the brains on day 21. The determination of tumor sizes from vibratome sections stained with cresyl violet revealed a reduction of tumor sizes in the specific treatment group by 39% or 25% compared to the untreated or negative control treated group, respectively (Figure 8, *B*). This was based on the profound knockdown of PLK1 expression in the specific treatment group, as determined by immunohistochemical analysis of paraffin sections of the gliomas (Figure 8, *C*, upper panel). Concomitantly, an increase in cleaved Caspase-3 was observed in the tumor tissue, indicating the induction of apoptosis upon PLK1 knockdown (Figure 8, *C*, lower panel). Since tumor cell invasion into the surrounding healthy tissue is a major issue in gliomas, contributing to poor resectability of the tumor and concomitant poor prognosis, we also analyzed the tumor boundaries with regard to signs of invasion. Indeed, tumor tissue boundaries were found much more even in the specific treatment group, indicating the absence of invasive properties and tumor cell dissemination from the bulk tumor mass as observed in the negative control groups (Figure 8, *D*).

Taken together, this demonstrates the therapeutic efficacy of LP10Y/siPLK1 complexes in three different xenograft or xenopatient tumor models, covering subcutaneous as well as orthotopic localization.

Discussion

Linear PEIs are preferred over their branched counterparts for several reasons, including higher biocompatibility and more defined chemical compositions, and are already explored in clinical studies aiming at gene delivery. However, their capacity for complexation and thus delivery of small RNA molecules is poor. Strikingly, we show that this is entirely changed upon tyrosine engraftment of the polymer. This approach is particularly appealing since it relies on a relatively simple and straightforward chemical modification, avoiding very complicated chemistries as seen in the case of certain liposomes developed for therapeutic siRNA delivery (*e.g.*, SNALPs). Thus, this offers a high potential for possible translation into the clinics.

Notably, our results demonstrate that the tyrosine-modification addresses, and positively affects, three important parameters in parallel: the complex stability, which is markedly enhanced and now sufficient for siRNA delivery, cellular uptake, which benefits from enhanced interaction of the polymer with the cell membrane, and intracellular siRNA release into the right compartment as another key process for siRNA activity. It is therefore by no means surprising that the tyrosine content is critical and requires some fine-tuning, with an ~30% degree of substitution found to be optimal. More specifically, while tyrosine-grafting leads to more stable complexes (which is beneficial and thus improves knockdown efficacy), higher degrees of tyrosine-modification may lead to complexes with non-optimal stability and/or less efficient uptake due to reduced surface charge. Thus, the optimal degree of tyrosine grafting seems to be crucial for balancing these different effects in a way that the optimal setting is achieved. This also highlights that, beyond the positive charges in the polymer required for (negatively charged) siRNA complexation, the presence of hydrophobic/aromatic components is very beneficial for complexation and improved physicochemical/biological complex properties. Thus, the positive effect of tyrosine grafting may rely on the contribution of others than electrostatic interactions, including π–π interactions. While this has already been suggested from previous studies on branched PEIs,[31,32,35] we now show that this is even more important for small linear PEIs which, as stated above, are preferred over their branched counterparts. In fact, only upon tyrosine modification did the linear PEIs become available for siRNA delivery. This is particularly relevant with regard to very small PEIs, since PEI cytotoxicity is generally correlated with polymer chain length. The polymer chain length of the best performing LP10Y is about 50% of the *in vivo* jetPEI already used in clinical gene delivery studies, and it is tempting to speculate that, for example by increasing siRNA molecular weights by using siRNA concatemers,[23] even smaller LP*x*Y may well show equal efficacy.

Another critical parameter is the cationic surface charge, which is associated with cytotoxicity and markedly reduced upon tyrosine modification. The variation of complexation conditions may be particularly relevant as well, especially when considering that we observed a very profound effect of buffer conditions on complex sizes. Comparably large complexes (*i.e.*, several hundred nm in diameter) still showed very profound transfection efficacy *in vitro*. This could indicate that complex sizes may not be critical for cellular internalization and siRNA delivery at least in cell culture. However, it has also been observed in cell culture that complexes based on linear PEI form aggregates under salt conditions[39] and may show unspecific transfection efficiency, possibly contributing as well. Furthermore, the optimal size of complexes is discussed controversially. While larger PEI/pDNA complexes often showed improved transfection efficiencies *in vitro* compared to their smaller counterparts,[40] most *in vivo* studies rather use smaller nanoparticles as perhaps more suitable with regard to tissue penetration upon systemic administration.[41] However, one paper also demonstrated the advantage of larger complexes *in vivo* for intratumoral injections in s.c. xenografts or in abdominal tumor models.[42] Still, for *in vivo* use smaller complexes will be preferred due to better tissue penetration. Beyond the *in vivo* therapy studies, our results from the *ex vivo* tissue slice experiments also indicate favorable tissue penetration since an overall ~50% target gene knockdown in the whole slice cannot be based just on biological activity on the outer cell layers. This notion is also supported by more recent findings in our group demonstrating tissue penetration of the complexes by immunohistochemistry (Karimov, Ewe and Aigner, unpublished). Notably, this is somewhat contradictory to other observations that suggest impaired tissue penetration already of single molecules, *e.g.*, biologicals or even small molecule cytostatics (see *e.g.*[43]). In fact, this may indicate the need for a delicate balance between cell uptake efficacy, which has to be sufficiently high for biological effects and adequately low for allowing deeper tissue penetration without interference only with the first cell layers hit after extravasation into their target tissue.

This also implicates that it is insufficient to evaluate a given nanoparticle only in 2D cell culture. Rather, it is pivotal to demonstrate efficacy in appropriate *in vivo* models. In this regard, PDX models are particularly relevant since they recapitulate tumor tissue architecture even after several rounds of propagation in mice, and orthotopic tumor models are advantageous in recapitulating most precisely the original tumor environment. Both aspects have been addressed in this study. In a therapeutic context, the systemic administration is preferable and therapeutically more relevant over local application, despite possible delivery to non-target tissues/organs. Thus, systemic application was the focus in this study. While in the case of subcutaneous tumor xenografts i.p. injection was preferred, a 'real patient tumor' situation may rather require i.v. administration. One exception from systemic treatment, however, may be gliomas, where – despite its partial impairment due to the tumor – the blood–brain barrier still presents a major hurdle for drug delivery, including nanoparticles. While the targeted delivery of nanoparticles through the blood–brain barrier has been a matter of intense research over decades, efficient systems are still lacking (see *e.g.*[44] for review) and our complexes based on LP10Y may not solve this problem. It should be noted, however, that direct intratumoral application, *e.g.* by convection-enhanced delivery, is clearly feasible in a clinical setting for treating glioma patients.[45]

Upon injection, in particular into the blood stream, nanoparticles experience the adsorption of proteins, which leads to the formation of the so-called "soft" and "hard corona", affecting nanoparticle properties (see *e.g.*[46,47] for review). As shown here, the presence of proteins did not impair complex efficacy and even protected complexes from aggregation. It is well feasible that complexes may benefit from this corona formation also upon systemic injection *in vivo*, and that altered chemical properties (here: tyrosine modification) will also determine alterations in the protein corona composition. Thus, beyond the positive effects of tyrosine modification on physicochemical complex properties described here, leading to enhanced biological efficacy, complexes may further benefit in the *in vivo* situation.

Acknowledgments

This study was supported by grants from the Deutsche Forschungsgemeinschaft (DFG; AI 24/21-1; AI 24/24-1) and the

Deutsche Krebshilfe (70111616) to A.A., and the NAWA IAP Program EUROPARTNER (M.B., M.I., A.A.). The authors are grateful to Markus Böhlmann and Anne-Kathrin Krause (both RBI) for expert mouse maintenance and assistance in the experiments, and to Katrin Becker for expert help with tissue slice experiments and immunohistochemistry.

Author contributions

Conceptualization, A.A., A.E., M.B.; Formal analysis, T.B., U. K., A.E., A.A.; Funding acquisition, A.A., M.B.; Investigation, M. K., T.K., S.N., M.K., A.R., M.S., T.K.; Project administration, A. A., A.E.; Resources, I.G., R.T., U.K.; Supervision, A.E., H.F., M. I., U.K., A.A.; Writing - original draft, M.K., A.E., A.A.; Writing - review & editing, A.A., A.E.

All authors have read and agreed to the published version of the manuscript.

Appendix A. Supplementary data

Supplementary data to this article can be found online at https://doi.org/10.1016/j.nano.2021.102403.

References

1. Fire A, Xu S, Montgomery MK, Kostas SA, Driver SE, Mello CC. Potent and specific genetic interference by double-stranded RNA in Caenorhabditis elegans. *Nature* 1998;**391**:806-11.
2. Elbashir SM, Harborth J, Lendeckel W, Yalcin A, Weber K, Tuschl T. Duplexes of 21-nucleotide RNAs mediate RNA interference in cultured mammalian cells. *Nature* 2001;**411**:494-8.
3. Elbashir SM, Lendeckel W, Tuschl T. RNA interference is mediated by 21- and 22-nucleotide RNAs. *Genes Dev* 2001;**15**:188-200.
4. Yin H, Kanasty RL, Eltoukhy AA, Vegas AJ, Dorkin JR, Anderson DG. Non-viral vectors for gene-based therapy. *Nat Rev Genet* 2014;**15**:541-55.
5. Videira M, Arranja A, Rafael D, Gaspar R. Preclinical development of siRNA therapeutics: towards the match between fundamental science and engineered systems. *Nanomedicine* 2014;**10**:689-702.
6. Wicki A, Witzigmann D, Balasubramanian V, Huwyler J. Nanomedicine in cancer therapy: challenges, opportunities, and clinical applications. *J Control Release* 2015;**200**:138-57.
7. Kim B, Park JH. Sailor MJ. Rekindling RNAi therapy: materials design requirements for in vivo siRNA delivery. *Adv Mater* 2019e1903637.
8. Boussif O, Lezoualc'h F, Zanta MA, Mergny MD, Scherman D, Demeneix B, et al. A versatile vector for gene and oligonucleotide transfer into cells in culture and in vivo: polyethylenimine. *Proc Natl Acad Sci U S A* 1995;**92**:7297-301.
9. Neu M, Fischer D, Kissel T. Recent advances in rational gene transfer vector design based on poly(ethylene imine) and its derivatives. *J Gene Med* 2005;**7**:992-1009.
10. Pandey AP, Sawant KK. Polyethylenimine: a versatile, multifunctional non-viral vector for nucleic acid delivery. *Korean J Couns Psychother* 2016;**68**:904-18.
11. Hobel S, Aigner A. Polyethylenimines for siRNA and miRNA delivery in vivo. *Wiley Interdiscip Rev Nanomed Nanobiotechnol* 2013.
12. Kafil V, Omidi Y. Cytotoxic impacts of linear and branched polyethylenimine nanostructures in a431 cells. *Bioimpacts* 2011;**1**:23-30.
13. Kwok A, Hart SL. Comparative structural and functional studies of nanoparticle formulations for DNA and siRNA delivery. *Nanomedicine* 2011;**7**:210-9.
14. Tauhardt L, Kempe K, Knop K, Altuntas E, Jäger M, Schubert S, et al. Linear polyethyleneimine: optimized synthesis and characterization — on the way to "pharmagrade" batches. *Macromol Chem Phys* 2011;**212**:1918-24.
15. von Harpe A, Petersen H, Li Y, Kissel T. Characterization of commercially available and synthesized polyethylenimines for gene delivery. *J Control Release* 2000;**69**:309-22.
16. Moreadith RW, Viegas TX, Bentley MD, Harris M, Fang Z, Yoon K, et al. Clinical development of a poly(2-oxazoline) (POZ) polymer therapeutic for the treatment of Parkinson's disease — proof of concept of POZ as a versatile polymer platform for drug development in multiple therapeutic indications. *Eur Polym J* 2017;**88**:524-52.
17. Buscail L, Bournet B, Vernejoul F, Cambois G, Lulka H, Hanoun N, et al. First-in-man phase 1 clinical trial of gene therapy for advanced pancreatic cancer: safety, biodistribution, and preliminary clinical findings. *Mol Ther* 2015;**23**:779-89.
18. Sidi AA, Ohana P, Benjamin S, Shalev M, Ransom JH, Lamm D, et al. Phase I/II marker lesion study of intravesical BC-819 DNA plasmid in H19 over expressing superficial bladder cancer refractory to bacillus Calmette-Guerin. *J Urol* 2008;**180**:2379-83.
19. Gofrit ON, Benjamin S, Halachmi S, Leibovitch I, Dotan Z, Lamm DL, et al. DNA based therapy with diphtheria toxin-A BC-819: a phase 2b marker lesion trial in patients with intermediate risk nonmuscle invasive bladder cancer. *J Urol* 2014;**191**:1697-702.
20. Lori F. DermaVir: a plasmid DNA-based nanomedicine therapeutic vaccine for the treatment of HIV/AIDS. *Expert Rev Vaccines* 2011;**10**:1371-84.
21. Kedinger V, Meulle A, Zounib O, Bonnet ME, Gossart JB, Benoit E, et al. Sticky siRNAs targeting survivin and cyclin B1 exert an antitumoral effect on melanoma subcutaneous xenografts and lung metastases. *BMC Cancer* 2013;**13**:338.
22. Hong CA, Nam YS. Reducible dimeric conjugates of small internally segment interfering RNA for efficient gene silencing. *Macromol Biosci* 2016;**16**:1442-9.
23. Bolcato-Bellemin AL, Bonnet ME, Creusat G, Erbacher P, Behr JP. Sticky overhangs enhance siRNA-mediated gene silencing. *Proc Natl Acad Sci U S A* 2007;**104**:16050-5.
24. Pinnapireddy SR, Duse L, Strehlow B, Schafer J, Bakowsky U. Composite liposome-PEI/nucleic acid lipopolyplexes for safe and efficient gene delivery and gene knockdown. *Colloids Surf B Biointerfaces* 2017;**158**:93-101.
25. Shim MS, Kwon YJ. Acid-responsive linear polyethylenimine for efficient, specific, and biocompatible siRNA delivery. *Bioconjug Chem* 2009;**20**:488-99.
26. Bansal R, Seth B, Tiwari S, Jahan S, Kumari M, Pant AB, et al. Hexadecylated linear PEI self-assembled nanostructures as efficient vectors for neuronal gene delivery. *Drug Deliv Transl Res* 2018;**8**:1436-49.
27. Patil S, Lalani R, Bhatt P, Vhora I, Patel V, Patela H, et al. Hydroxyethyl substituted linear polyethylenimine for safe and efficient delivery of siRNA therapeutics. *RSC Adv* 2018;**8**:35461.
28. Endres T, Zheng M, Beck-Broichsitter M, Samsonova O, Debus H, Kissel T. Optimising the self-assembly of siRNA loaded PEG-PCL-lPEI nano-carriers employing different preparation techniques. *J Control Release* 2012;**160**:583-91.
29. Aldawsari H, Edrada-Ebel R, Blatchford DR, Tate RJ, Tetley L, Dufes C. Enhanced gene expression in tumors after intravenous administration of arginine-, lysine- and leucine-bearing polypropylenimine polyplex. *Biomaterials* 2011;**32**:5889-99.
30. Yu W, Zheng Y, Yang Z, Fei H, Wang Y, Hou X, et al. N-AC-l-Leu-PEI-mediated miR-34a delivery improves osteogenic differentiation under orthodontic force. *Oncotarget* 2017;**8**:110460-73.
31. Creusat G, Zuber G. Self-assembling polyethylenimine derivatives mediate efficient siRNA delivery in mammalian cells. *Chembiochem* 2008;**9**:2787-9.

32. Creusat G, Zuber G. Tyrosine-modified PEI: a novel and highly efficient vector for siRNA delivery in mammalian cells. *Nucleic Acids Symp Ser (Oxf)* 2008:91-2.
33. Creusat G, Rinaldi AS, Weiss E, Elbaghdadi R, Remy JS, Mulherkar R, et al. Proton sponge trick for pH-sensitive disassembly of polyethylenimine-based siRNA delivery systems. *Bioconjug Chem* 2010;**21**:994-1002.
34. Ewe A, Noske S, Karimov M, Aigner A. Polymeric nanoparticles based on tyrosine-modified, low molecular weight polyethylenimines for siRNA delivery. *Pharmaceutics* 2019;**11**.
35. Ewe A, Przybylski S, Burkhardt J, Janke A, Appelhans D, Aigner A. A novel tyrosine-modified low molecular weight polyethylenimine (P10Y) for efficient siRNA delivery in vitro and in vivo. *J Control Release* 2016;**230**:13-25.
36. Brockmann MA, Westphal M, Lamszus K. Improved method for the intracerebral engraftment of tumour cells and intratumoural treatment using a guide screw system in mice. *Acta Neurochir* 2003;**145**:777-81 discussion 781.
37. Mahammad S, Parmryd I. Cholesterol depletion using methyl-beta-cyclodextrin. *Methods Mol Biol* 2015;**1232**:91-102.
38. Schlingensiepen KH, Schlingensiepen R, Steinbrecher A, Hau P, Bogdahn U, Fischer-Blass B, et al. Targeted tumor therapy with the TGF-beta2 antisense compound AP 12009. *Cytokine Growth Factor Rev* 2006;**17**:129-39.
39. Wightman L, Kircheis R, Rossler V, Carotta S, Ruzicka R, Kursa M, et al. Different behavior of branched and linear polyethylenimine for gene delivery in vitro and in vivo. *J Gene Med* 2001;**3**:362-72.
40. Pezzoli D, Giupponi E, Mantovani D, Candiani G. Size matters for in vitro gene delivery: investigating the relationships among complexation protocol, transfection medium, size and sedimentation. *Sci Rep* 2017;**7**:44134.
41. Prabha S, Arya G, Chandra R, Ahmed B, Nimesh S. Effect of size on biological properties of nanoparticles employed in gene delivery. *Artif Cells Nanomed Biotechnol* 2016;**44**:83-91.
42. Zhang W, Kang X, Yuan B, Wang H, Zhang T, Shi M, et al. Nano-structural effects on gene transfection: large, botryoid-shaped nanoparticles enhance DNA delivery via macropinocytosis and effective dissociation. *Theranostics* 2019;**9**:1580-98.
43. Bockelmann L. *Starzonek C*. Karst U, Thomale J, Schluter H, et al. Detection of doxorubicin, cisplatin and therapeutic antibodies in formalin-fixed paraffin-embedded human cancer cells. *Histochem Cell Biol*: Niehoff AC; 2020.
44. Aigner A, Kogel D. Nanoparticle/siRNA-based therapy strategies in glioma: which nanoparticles, which siRNAs? *Nanomedicine (Lond)* 2018;**13**:89-103.
45. Bogdahn U, Hau P, Stockhammer G, Venkataramana NK, Mahapatra AK, Suri A, et al. Targeted therapy for high-grade glioma with the TGF-beta2 inhibitor trabedersen: results of a randomized and controlled phase IIb study. *Neuro Oncol* 2011;**13**:132-42.
46. Pederzoli F, Tosi G, Vandelli MA, Belletti D, Forni F, Ruozi B. Protein corona and nanoparticles: how can we investigate on? *Wiley Interdiscip Rev Nanomed Nanobiotechnol* 2017;**9**.
47. Mishra RK, Ahmad A, Vyawahare A, Alam P, Khan TH, Khan R. Biological effects of formation of protein corona onto nanoparticles. *Int J Biol Macromol* 2021;**175**:1-18.

Suppl. Figure 1 **(A)** NMR spectrum of a tyrosine-modified PEI with peak annotation. **(B)** Degrees of tyrosine-grafting obtained for the different linear PEIs with MW 2.5-25 kDa.

Suppl. Figure 2 **(A)** Heparin displacement assay for the assessment of complex stability in the presence of increasing concentrations of heparin and with (right) or without 50% FCS (left). Arrow: free siRNA. **(B)** Time-dependent microscopic analysis of the uptake of LP10Y-complexed, DY647-labeled siRNA in H441 cells. **(C)** Measurement of the concentration dependent interaction of LP10Y with extrinsic membrane probes, as determined by membrane fluidity analyses via fluorescence anisotropy with 1,6-diphenylhexatriene (DPH; left) or its trimethylammonium derivative (TMA-DPH; right).

Suppl. Figure 3 **(A)** Biological knockdown efficacies of complexes based on the various tyrosine-modified PEIs in H441-luc cells. Black and gray bars: complexes containing non-specific and luciferase-specific siRNAs, respectively, at two different siRNA amounts. **(B)** LP10Y/siRNA knockdown efficacies at different polymer/siRNA mass ratios.

Suppl. Figure 4 **(A)** Biological knockdown efficacies of complexes based on the various tyrosine-modified PEIs in different reporter cell lines. **(B)** Time-dependence of reporter gene knockdown.

Suppl. Figure 5 **(A)** Absence of apoptosis induction upon transfection of cells with complexes based on LP5Y or LP10Y, as determined by Caspase-3/-7 activity at different time points after transfection. **(B)** COMET assay for the determination of genotoxicity. Left: quantitation of tail moments indicating genotoxic events; right: representative pictures (two for each condition). Arrow: one positive event upon treatment with complexes based on linear 10 kDa PEI.

Suppl. Figure 6 **(A)** Dependence of biological knockdown efficacies on the duration of transfection. Black and gray bars: complexes containing non-specific and luciferase-specific siRNAs, respectively. **(B)** Knockdown efficacies in the presence of various inhibitors of cellular internalization at different concentrations. **(C)** Cell uptake of LP10Y-complexed, DY647-labeled siRNA in the presence of various inhibitors of cellular internalization, as determined by flow cytometry.

Suppl. Figure 7 Autoradiography results from a radioactive biodistribution experiment, 4 h after i.v. injection of complexes containing [32P]-labeled siRNA.

Suppl. Figure 8 Microscopic pictures of different organs from mice receiving repeated LP10Y/siRNA treatment (s.c. tumor xenograft experiment; see Figure 6) vs. untreated, hematoxylin or hematoxylin/eosin staining; bar: 200 pixels.

Q20 Suppl. Figure 9

Suppl. Table 1 siRNA used in this study.

Suppl. Table 2 Sequences of primers used in this study.

Suppl. Table 3 Antibodies used in this study.

Suppl. Table 4 1H-NMR (400 MHz, deuterium oxide) data.

Q21 Supplementary material

AUTHOR QUERY FORM

ELSEVIER	**Journal: NANO** **Article Number: 102403**	**Please e-mail your responses and any corrections to:** **E-mail: Corrections_ESCH.elsevier@spi-global.com**

Dear Author,

Please check your proof carefully and mark all corrections at the appropriate place in the proof (e.g., by using on-screen annotation in the PDF file) or compile them in a separate list. Note: if you opt to annotate the file with software other than Adobe Reader then please also highlight the appropriate place in the PDF file. To ensure fast publication of your paper please return your corrections within 48 hours.

For correction or revision of any artwork, please consult http://www.elsevier.com/artworkinstructions.

We were unable to process your file(s) fully electronically and have proceeded by

☐ Scanning (parts of) your article ☐ Rekeying (parts of) your article ☐ Scanning the artwork

Any queries or remarks that have arisen during the processing of your manuscript are listed below and highlighted by flags in the proof. Click on the 'Q' link to go to the location in the proof.

Location in article	**Query / Remark: click on the Q link to go** **Please insert your reply or correction at the corresponding line in the proof**
Q1	Your article is registered as a regular item and is being processed for inclusion in a regular issue of the journal. If this is NOT correct and your article belongs to a Special Issue/Collection please contact j.m.francis@elsevier.com immediately prior to returning your corrections.
Q2	The author names have been tagged as given names and surnames (surnames are highlighted in teal color). Please confirm if they have been identified correctly.
Q3, Q5, Q6, Q7, Q8, Q9, Q10, Q11, Q12, Q13, Q14, Q15, Q16, Q17, Q18	Professional Degree (e.i., PhD, MD, MSc, etc.) is mandatory for this journal. Please check and provide.
Q4	Please indicate each author's academic degree.
Q19	Data may have been inadvertently omitted here (upon?). Please check.
Q20	Please provide caption.
Q21	Supplementary caption was not provided. Please check the suggested data if appropriate, and correct if necessary.
Q22	Correctly acknowledging the primary funders and grant IDs of your research is important to ensure compliance with funder policies. We could not find any acknowledgement of funding sources in your text. Is this correct?
Q23	Please provide the volume number and page range for the bibliography in Ref. 7..

Q24	Please provide the volume number and page range for the bibliography in Ref. 11.. Please check this box if you have no corrections to make to the PDF file. ☐

Thank you for your assistance.